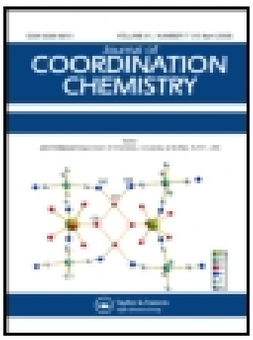

Journal of Coordination Chemistry

ISSN: 0095-8972 (Print) 1029-0389 (Online) Journal homepage: http://www.tandfonline.com/loi/gcoo20

Mononuclear oxidodiperoxido vanadium(V) complex: synthesis, structure, VHPO mimicking oxidative bromination, and potential detection of hydrogen peroxide

Haimanti Adhikari & Kalyan K. Mukherjea

To cite this article: Haimanti Adhikari & Kalyan K. Mukherjea (2018): Mononuclear oxidodiperoxido vanadium(V) complex: synthesis, structure, VHPO mimicking oxidative bromination, and potential detection of hydrogen peroxide, Journal of Coordination Chemistry, DOI: 10.1080/00958972.2018.1439936

To link to this article: https://doi.org/10.1080/00958972.2018.1439936

JOURNAL OF COORDINATION CHEMISTRY, 2018
https://doi.org/10.1080/00958972.2018.1439936

Taylor & Francis
Taylor & Francis Group

Mononuclear oxidodiperoxido vanadium(V) complex: synthesis, structure, VHPO mimicking oxidative bromination, and potential detection of hydrogen peroxide

Haimanti Adhikari and Kalyan K. Mukherjea

Department of Chemistry, Jadavpur University, Kolkata, India

ABSTRACT

An oxidodiperoxidovanadium(V) complex, $(NH_4)[VO(O_2)_2(phen)](H_2O)_2$, has been synthesized and structurally characterized. The complex crystallizes in the $P2_1/c$ space group. The vanadium center is seven-coordinate with pentagonal bipyramidal geometry. The compound was designed in order to develop a VHPO mimic, so it was tested for VHPO activity through the single pot bromination of phenol red to bromophenol blue whereby, it afforded positive response to establish that the complex is indeed a VHPO mimic. In addition, the compound is capable of detection of H_2O_2.

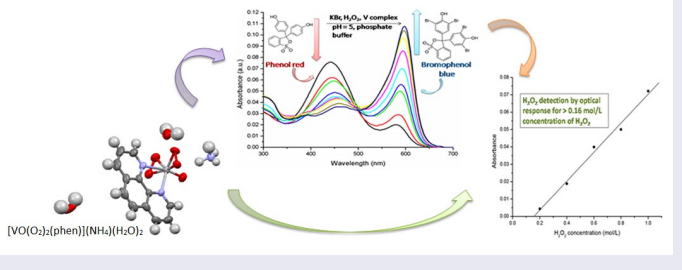

ARTICLE HISTORY
Received 7 August 2017
Accepted 26 January 2018

KEYWORDS
Oxidodiperoxido vanadium complex; structure; bromoperoxidation catalysis; H_2O_2 detection

1. Introduction

Vanadium haloperoxidase (VHPO) is the first isolated vanadium-dependent enzyme from the marine algae *Ascophyllum nodosum*. In 1984 and later, it was found in some lichens and other marine algae as well [1, 2]. Vanadium-containing complexes have obtained attention due to their wide biological and catalytic properties such as haloperoxidation, nitrogen fixation, metalloprotein function, insulin-mimicking activities [3, 4]. The incorporation of halogen atoms in many organic compounds by nature leads to the formation of halogenated antibiotics, drugs, or signaling molecules in biological systems [5]. Halogenated compounds,

CONTACT Kalyan K. Mukherjea k_mukherjea@yahoo.com, kkmukherjee@chemistry.jdvu.ac.in
The supplementary material for this article is available online at https://doi.org/10.1080/00958972.2018.1439936.

usually found in marine organisms, especially marine macroalgae, seem to be important factors of halogen transfers in the coastal marine environment [6–8]. Among halogenating enzymes, haloperoxidases utilize hydrogen peroxide for electrophilic halogenation via the oxidation of halides [5, 9–12].

Vanadium-dependent haloperoxidase (VHPO) enzymes show antioxidant activity and are believed to take part in chemical defense in some biological systems [13,14]. VHPOs are classified according to the most electronegative halide that they can oxidize, *i.e.* chloroperoxidases (VCPO) can catalyze the oxidation of chloride as well as of bromide and iodide, and bromoperoxidases (VBPO) react with bromide and iodide, whereas iodoperoxidases (VIPO) are specific for iodide. Until recently, only chloro- and bromoperoxidases from eukaryotic species have been studied, showing a fragmental view of this large enzyme family. Novel types of VHPO discovered in marine bacteria now give some clues to explore new biosynthetic pathways of natural halogenated compounds through *in vitro* heterologous expression. Further studies on the structure–function relationships in the catalytic and specificity mechanism are warranted to shed light on the evolution of the VHPO family.

These VHPOs can halogenate particular substrates in phenyl rings [15]. It has been reported earlier that VHPOs oxidize the halide ion through coordinating hydrogen peroxide; the nature of the oxidized halide species seems to depend on the nature of the organic substrate. Then halogenation of appropriate organic substrate occurs by these oxidized halogen species. They can also oxidize a second equivalent of hydrogen peroxide, producing dioxygen [16]. The main active center of VHPO has been reported to contain a VO_4N moiety [17]. Although the mechanism of VHPO is not yet fully established, in order to explore the relationship between the structure and the catalytic activity of the enzyme mimics, a large number of vanadium complexes have been synthesized [18–20]. Extracted VHPO enzyme also was tested *in vitro* for the bromination reaction of phenol red to understand its mechanism [21]. As a peroxido group is present in the active site, peroxidovanadium compounds are considered to be more effective to mimic the VHPO system. So the present work has been undertaken to develop compounds containing peroxidovanadium moiety. Accordingly, a compound, $[VO(O_2)_2(phen)](NH_4)(H_2O)_2]$, has been synthesized, whose characterization was undertaken using UV–vis spectroscopy, IR, NMR, mass spectroscopy, and X-ray crystallography.

Because of some unique properties, hydrogen peroxide has been used for years in various fields [22]. So, determination of H_2O_2 has a great practical importance. Although there are several methods of detection of it, the colorimetric method of assay appears to be more cost effective and simple [23–25]. Envisaging the simplicity of metal complex-based methods, we concentrated our attention to develop a simple H_2O_2 sensing model system with the peroxido vanadium complex. Eventually, the complex was found to act both as a VHPO mimic as well as a H_2O_2 sensing agent.

2. Experimental

2.1. Materials

Ammonium metavanadate (NH_4VO_3) was obtained from S.D. Fine Chem. Ltd. (India). Extra pure varieties of 1,10-phenanthroline, hydrogen peroxide (30% w/v), phenol red, and methanol (G.R.) were the products of E. Merck (India) and were used directly. All other reagents

used were of analytical grade. The analytical grade solvents used for physicochemical studies were further purified before use wherever necessary, by literature methods [26].

2.2. Synthesis of the metal complex $(NH_4)[VO(O_2)_2(phen)](H_2O)_2$

Ammonium metavanadate (0.117 g, 1 mmol) was dissolved in 1.0 mL of hydrogen peroxide taken in a beaker and placed in an ice bath at 0–5 °C, and the pH of the resulting solution was made 3 by adding dilute HNO_3. In a separate beaker, the ligand (1,10-phenanthroline) (0.198 g, 1 mmol) was dissolved in methanol and the solution was added dropwise to the ammonium metavanadate solution in hydrogen peroxide with constant stirring. After the addition was complete, the mixture was stirred for about 2 h resulting in a yellow solution which was filtered and the filtrate was kept at 4 °C for slow evaporation. Yellow needle-shaped crystals of *ammoniumdiaqua oxidodiperoxidophenanthrolinevanadate(V)* separated out ($[VO(O_2)_2(phen)](NH_4)(H_2O)_2$) after a few days. Yield: 0.2217 g, 61%. IR (KBr, pellet, cm^{-1}): 1517 m (vC–C), 1426s, 724s (vC–N), 926s (vO–O), 622s, 584s (vV–O). UV–vis (H_2O) = 224, 271 (λ_{max}), 293 nm. ES mass (m/z): 365.09 (Figure S2).

2.3. X-ray structure

The crystal structure of the vanadium complex was determined by single-crystal X-ray diffraction. All geometric and intensity data were collected at room temperature using an automated Bruker SMART APEX-II diffractometer equipped with a CCD detector and fine focus 1.75 kW sealed tube Mo Kα X-ray source (λ = 0.71073 Å) [27]. All data were corrected for Lorentz and polarization effects [27]. The data were processed using SAINT and absorption corrections were made using SADABS [27]. Structures were solved by the combination of Patterson and Fourier techniques and refined by full-matrix least-square method using the SHELX suite of programs [28a]. All hydrogens belonging to **1** were placed in their calculated positions and refined using a riding model. Anisotropic refinement was carried out for all non-hydrogen atoms. Perspective views of the molecules were obtained by Mercury [28b] and ORTEP3 [28c].

The X-ray crystallographic data (CIF file) for the structure reported in this paper have been deposited in the Cambridge Crystallographic Data Center (CCDC) and the deposition number is CCDC 1533513.

2.4. Physical measurements for the characterization of the complexes

UV–vis spectra were recorded on a Shimadzu U-1800 spectrophotometer; IR spectra (KBr disk) were recorded on a Perkin Elmer IR spectrophotometer. Electrical conductivity of a 10^{-3} M dm^{-3} aqueous solution of the complex was measured with a Systronics 304 digital conductivity meter. Magnetic susceptibility measurements were made with a vibrating sample magnetometer PAR 155 model. All pH measurements were made with an Elico (India) digital pH meter. The mass spectral analyses were done using a mass spectrometer (model: XEVO-G2QTOF#YCA351).

2.5. Assessment of bromination activity

The bromination reaction was carried out in an aqueous medium at 30 ± 0.5 °C. The reactions involving bromide were performed under constant temperature. Solutions used for kinetic measurements were maintained at a constant concentration of H^+ (pH = 5.0) by the addition of NaH_2PO_4–Na_2HPO_4 [29]. The rate of this reaction is described by the rate law $dc/dt = kc_1^x c_2^y c_3^z$, and the equation of log (d*c*/d*t*) = log*k* + *x*logc_1 + *y*logc_2 + *z*logc_3 is obtained. It corresponds to –log (d*A*/d*t*) = –*x*logc_1–*b* (*b* = log*k* + *y*logc_2 + *z*logc_3), where A is the measurable absorbance of the resultant solution; *k* is the reaction rate constant; c_1, c_2, c_3 are the concentrations of the vanadium complex, KBr and phenol red, respectively; while *x*, *y*, *z* are the corresponding reaction orders. A plot of absorbance data at 592 nm *versus* time gave a straight line and from the slope of this line the reaction rate of the oxidovanadium complex (d*A*/d*t*) was obtained. By changing the concentration of the complex, a series of d*A*/d*t* data were obtained and from a plot of –log (d*A*/d*t*) *versus* –logc_1 the reaction rate constant (*k*) was calculated.

3. Results and discussion

The aim of the present work is to develop a bromoperoxidase mimic, one of the demanding fields of biochemical research. The strategy adopted to attain the goal is to synthesize the oxidodiperoxidovanadium(V) complex followed by examining the catalytic bromination of phenol red to bromophenol blue and subsequent exploitation of the compound in H_2O_2 sensing.

3.1. Synthetic aspects of the complex

Although the synthesis of an oxidodiperoxido vanadium complex with 1,10-phenanthroline was reported earlier, no mention of the structurally characterized mononuclear oxidodiperoxido vanadium compound with 1,10-phenanthroline could be found in literature [30]. We have been successful in characterizing the oxidodiperoxido vanadium compound $(NH_4)[VO(O_2)_2(phen)](H_2O)_2$ structurally and the crystal data are reported in the present work. The complexes were synthesized following Scheme 1.

3.2. Crystal structure of the complex

Single-crystal X-ray diffraction analysis (Table 1) reveals that the complex crystallizes in the monoclinic $P2_1/c$ space group. An ORTEP view of the asymmetric unit of the complex is shown in Figure 1. The crystal structure of the oxidodiperoxido vanadium complex consists of a discrete monomeric anionic unit, $[VO(O_2)_2(phen)]$, with an ammonium moiety as counter cation. Two H_2O molecules are also found in the crystal lattice. In this complex, the vanadium atom is surrounded with a N_2O_5 coordination sphere which is defined by one neutral bidentate ligand 1,10-phenanthroline (phen) (N, N donors), two peroxido, and an oxido moiety.

One of the two ring-nitrogen atoms of the neutral bidentate phen ligand, N2, occupies the equatorial plane together with the two peroxido groups of oxygen atoms O1, O2, O3, O4. The coordination environment around the vanadium can be described as a distorted seven-coordinate pentagonal-bipyramid. The axial positions of the coordination sphere are occupied by the oxido group O5 and one ring-nitrogen atom N1 of the bidentate ligand

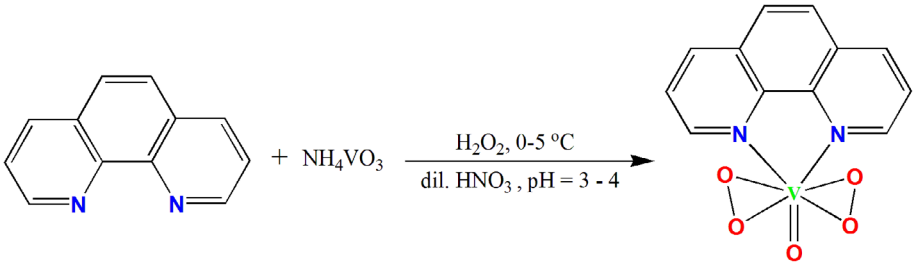

Scheme 1. Schematic representation for the preparation of the complex.

Table 1. X-ray diffraction analysis data of complexes.

Parameter	Complex
Empirical formula	$C_{12}H_{16}N_3O_7V$
M	365.22
T/K	373
λ/Å	0.71073
Crystal system	Monoclinic
Space group	*P 1 21/c 1*
Unit cell dimensions	
a/Å	7.0581(4)
b/Å	13.5897(7)
c/Å	16.5083(9)
α/°	90
β/°	96.242(4)
γ/°	90
V/ Å^3	1574.05(15)
Z, *D*/g cm^{-3}	4, 1.541
F(000)	752
Crystal size/mm	0.2 × 0.1 × 0.08
2θ range for data collection (°)	3.9 to 55.34
Reflection	25,888
Independent reflections (Rint)	3671, 0.0838
Completeness to $\theta = \theta_{max}$ (%)	100
Linear absorption coefficient *μ* (mm^{-1})	0.669
Refinement method	Full-matrix least-squares on F^2
Data / restraints / parameters	3671 / 4 / 230
Goodness-of-fit on F^2	0.989
Final R indices [$I > 2\sigma(I)$]	R1 = 0.0562, wR2 = 0.1408
R indices (all data)	R1 = 0.1065, wR2 = 0.1645
Largest diff. peak, hole/Å^3	0.50, −0.43

1,10-phen. Butler has already established that generally vanadium with an oxidodiperoxido arrangement and with one bidentate or two monodentate ligands crystallizes in a distorted pentagonal bipyramidal geometry [16]. A similar kind of structure with a different ligand system has been reported earlier [31]. The structural parameters are consistent with other vanadium(V) oxido-peroxido complexes which generally feature the vanadium atom coordinated to an oxido atom in an axial position and the peroxide group bound in the equatorial positions [32]. The length of the oxido V–O5 double bond is 1.609(3) Å, which is consistent with values found in other typical oxidovanadium(V) complexes [33]. The *trans* effect can be observed in the elongation of the apical coordinated N1 of the bidentate phen ligand (V1–N1) bond [2.336(3) Å], compared with the equatorial V1–N2 distance [2.152(3) Å]. Again,

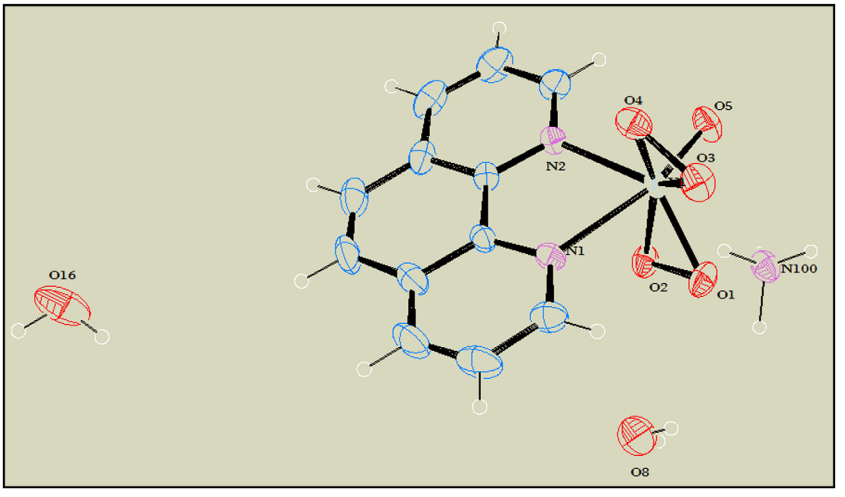

Figure 1. ORTEP view of the structure of the complex with ellipsoids at 30% probability.

the V1–N2 bond distance [2.152(3) Å] is longer than the V1–O1, V1–O2, V1–O3, and V1–O4 bond distances (1.869(3), 1.902(3), 1.870(3), and 1.923(3) Å, respectively) due to the *trans* effect of the oxygen atoms of two η^2-peroxido ligands. The equatorial V–O (peroxido) bonds have comparable lengths as above mentioned values, with O–O bond distances of 1.461(3) Å (O1–O2) and 1.449(4) Å (O3–O4) while the O1–V1–O2 and O3–V1–O4 angles are 45.60(10)° and 44.90(11)°, respectively. The O5–V1–O3–O4 and O5–V1–O1–O2 torsion angles are 90.92(17) and −90.29(16), respectively. The bidentate neutral 1,10-phen ligand binds the metal forming one five-membered chelate ring at the vanadium center with the corresponding bite angle of 73.05(10)° (N1–V1–N2). The relevant bond lengths and angles are presented in Table 2. Hydrogen bonds are present in between two asymmetric units and are shown in Figure 2. Extended interactions are avoided for clarity.

3.3. IR and UV–vis spectroscopic characterization of the complex

The characteristic IR spectra of oxidodiperoxidovanadium complexes usually show sharp bands in the 942–970 cm^{-1} region due to the ν(V=O) [34] mode and the four bands can be expected corresponding to normal vibrations involving the $(O_2)V(O_2)$ group because of vanadium – peroxo oxygen-stretching vibrations (ν_1, ν_2, ν_3 and ν_4 (V–Op)) (Op = peroxo oxygen) [35]. For these kinds of systems, the ν_1 and ν_2 (V–Op) vibrations occur at approximately $\nu \sim$ 630 cm^{-1} and the ν_3 and ν_4 (V–Op) vibrations occur at about $\nu \sim 520$ cm^{-1} for symmetric and antisymmetric stretching, respectively [35]. But, in the case of pentagonal bipyramidal structures, ν_1 and ν_2 (V–Op) vibrations and ν_3 and ν_4 (V–Op) vibrations occur at $\nu = 620$ and $\nu = 590$ cm^{-1}, respectively [35]. Hence, the present findings of the appearance of the ν_1 and ν_2 vibrations at $\nu = 622$ cm^{-1} and ν_3 and ν_4 vibrations appear at $\nu = 584$ cm^{-1} support the presence of the (O2)V(O2) group and pentagonal bipyramidal geometry.

A strong band is at $\nu = 926$ cm^{-1} for the O–O intra-stretching mode of the V (O2) group. A low-intensity stretch ν(V=O) is positioned at 955 cm^{-1}. The strong vibration bands at 1517 cm^{-1} and 1426 cm^{-1}, 724 cm^{-1} are due to the C–C and C–N vibration of the ligand in the complex, respectively.

Table 2. Selected bond lengths (Å) and angles (°) of the complex.

Bond lengths (Å)					
V1–O1	1.868(3)	V1–O2	1.902(2)	V1–N1	2.334(3)
V1–N2	2.153(3)	V1–O5	1.610(2)	V1–O3	1.868(2)
V1–O4	1.923(3)	O1–O2	1.464(3)	O3–O4	1.450(4)
N1–C10	1.312(4)	N1–C11	1.361(4)	N2–Cl	1.322(4)
N2–C12	1.356(4)	C10–C9	1.414(6)	C9–C8	1.362(7)
C8–C7	1.380(6)	C7–C11	1.408(5)	C7–C6	1.446(6)
C11–C12	1.421(5)	C12–C4	1.412(4)	C1–C2	1.384(5)
C2–C3	1.347(6)	C3–C4	1.397(6)	C4–C5	1.420(5)
				C5–C6	1.317(6)
Bond angles (°)					
O1–V1–O2	45.68(10)	O1–V1–N1	85.90(11)	O1–V1–N2	128.94(11)
O1–V1–O4	132.16(11)	O2–V1–N1	79.10(10)	O2–V1–N2	84.27(10)
O2–V1–O4	158.45(11)	N2–V1–N1	73.10(10)	O5–V1–O1	104.36(13)
O5–V1–O2	100.05(13)	O5–V1–N1	164.97(12)	O5–V1–N2	91.87(12)
O5–V1–O3	104.41(12)	O5–V1–O4	100.78(12)	O3–V1–O1	89.22(12)
O3–V1–O2	133.02(12)	O3–V1–N1	86.42(11)	O3–V1–N2	133.44(12)
O3–V1–O4	44.97(11)	O4–V1–N1	79.35(10)	O4–V1–N2	89.60(11)
O2–O1–V1	68.40(13)	O1–O2–V1	65.92(13)	O4–O3–V1	69.52(14)
O3–O4–V1	65.51(14)	C10–N1–V1	129.7(3)	C11–N1–V1	112.7(2)

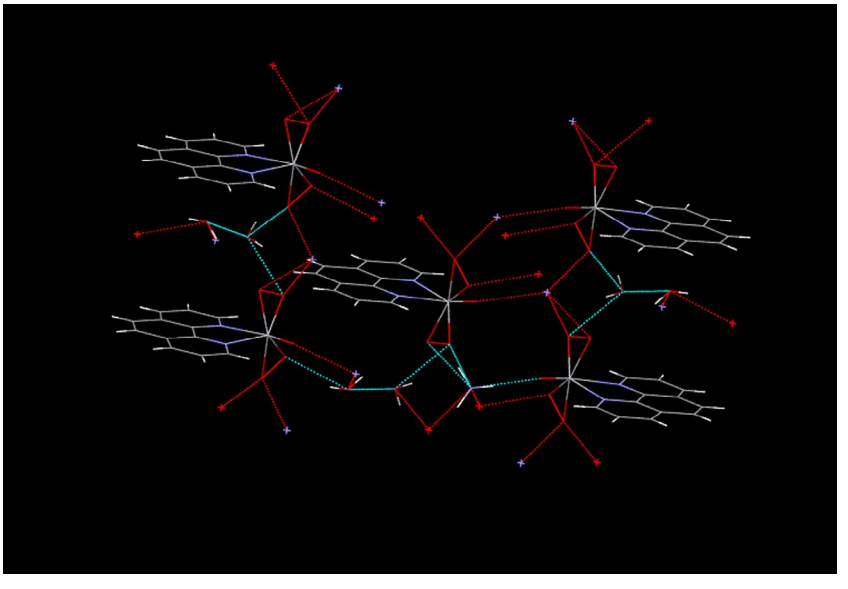

Figure 2. POV-ray image of H-bonding between different asymmetric units in wireframe presentation.

The electronic spectrum of the vanadium compound exhibits λ_{max} at 224 nm (ε = 14,460 M^{-1} cm^{-1}). This is due to the LMCT transition of $O_2^{2-} \rightarrow$ vanadium(V); the shoulder at 293 nm (ε = 3990 M^{-1} cm^{-1}) and a strong band at 271 nm (ε = 11,120 M^{-1} cm^{-1}) maybe assigned as the intra ligand $\pi \rightarrow \pi^*$ transitions of the aromatic ring of the coordinated ligand.

The mass spectral results also support the formulation of the complexes (see synthesis of the complexes).

3.4. Bromination activity for mimicking V-HPOs

The $[VO(O_2)]^+$ core of the peroxovanadium(V) complex $(NH_4)[VO(O_2)_2(phen)](H_2O)_2$ is to some extent equivalent to the respective mono-peroxovanadium(V) intermediate species of the VHPO enzymes which plays a key role in the enzymatic processes [36–40] in the presence of H_2O_2. Herein, the catalytic bromination activity of the complex has been tested using phenol red as substrate, which is characterized by the conversion of phenol red to bromophenol blue. The reaction is rapid and stoichiometric. The reaction process is presented in Scheme 2.

Addition of the solution of the vanadium complex to the standard reaction of bromide, in a phosphate buffer with phenol red as a trap for oxidized bromine, resulted in change in color of the solution from yellow to blue. The electronic absorption showed a decrease in absorbance of the peak at 443 nm for the loss of phenol red and an increase of the peak at 592 nm with production of bromophenol blue (shown in Figure 3).

3.4.1. Kinetic studies of bromination

To understand the kinetics of this reaction, the reaction was followed in aqueous medium at 30 ± 0.5 °C and was monitored by a gradual change in the concentration of the complex. The rate of this reaction is expressed by the rate law $dc/dt = kc_1^x c_2^y c_3^z$. According to the Beer–Lambert law, $A = \varepsilon dc$, which on differentiation we get $dA/dt = \varepsilon d(dc/dt)$. Then, the equation $-\log(dA/dt) = -x\log c_1 - b$ ($b = \log k + y\log c_2 + z\log c_3$) is obtained ($\varepsilon$, the molar absorption coefficient, for bromophenol blue = 14 500 M^{-1} cm^{-1} at 592 nm; '*d*' is the light path length of the sample cell ($d = 1$)), where A is the measurable absorbance of bromophenol blue at 592 nm, *k* is the reaction rate constant, and c_1, c_2, c_3 are the concentrations of the vanadium complex, KBr and phenol red, respectively; *x*, *y*, *z* are the corresponding orders of the reaction. Plots of absorbance data at 592 nm *versus* time for various concentration of the complex gave straight lines and from the slopes of these lines a series of reaction rates of the complex (dA/dt) were obtained (Figure 4). From Figure 4, it has been observed that after ~75 min, the rate of reaction increases slowly which can be supported by the visible difference in the respective absorbance values. The plot of $-\log(dc/dt)$ *versus* $-\log c$

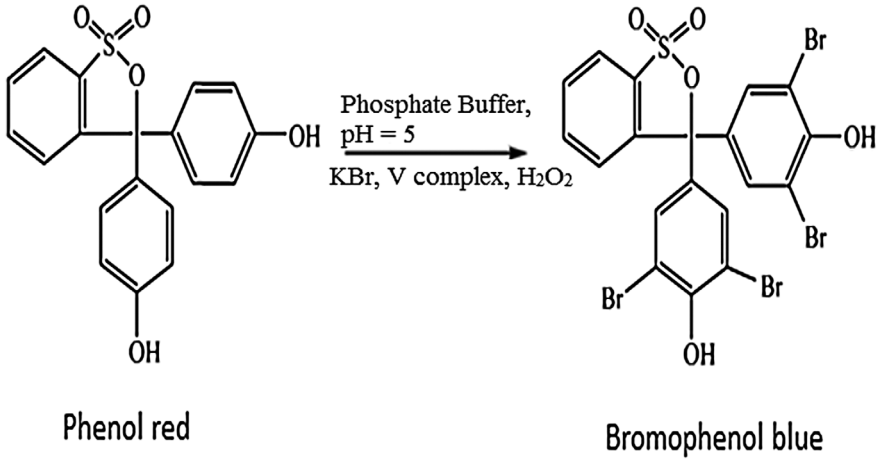

Scheme 2. The reactive process of bromination reaction for the complex.

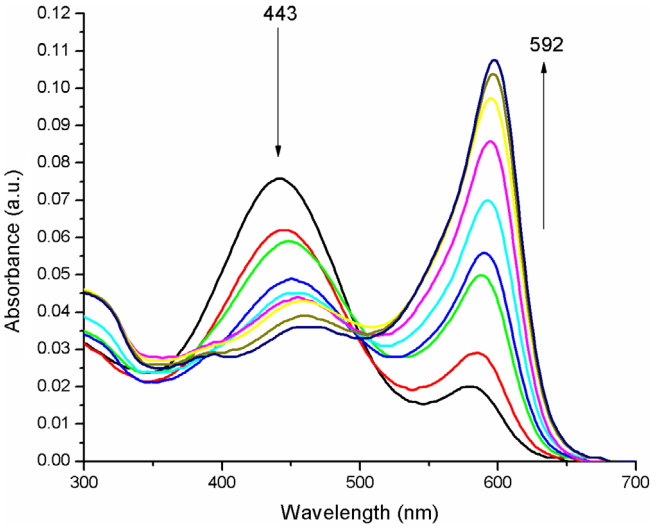

Figure 3. Oxidative bromination of phenol red catalyzed by the oxidovanadium complex (0.02 mmol). Spectral changes at 10 min intervals. Spectral data taken of aliquots in pH = 5.0 aqueous phosphate buffer, c(phosphate buffer) = 50 mmol L^{-1}, c(KBr) = 0.4 mol L^{-1}, c(phenol red) = 0.1 mmol L^{-1}.

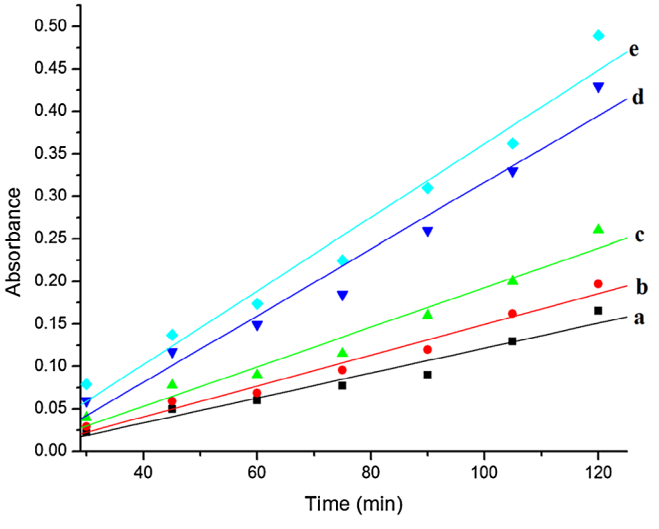

Figure 4. A series of linear calibration plots of the absorbance at 592 nm dependence of time for different concentrations of complex. Conditions used: pH 5.0, c(KBr) = 0.4 M L^{-1}, c(H_2O_2) = 0.02 M L^{-1}, c(phenol red) = 10^{-4} M L^{-1}. c(complex **2**/M L^{-1}) = a: 1×10^{-6}; b: 2.15×10^{-6}; c: 3.23×10^{-6}; d: 4.31×10^{-6}; e: 5.38×10^{-6}.

(Figure 5) gives a straight line with a slope of 1.0276 and an intercept of 2.0224. The orders of the reaction with respect to KBr and phenol red (*y* and *z*) are considered to be 1 according to the literature [41]; c_2 and c_3 are known to be 0.4 and 10^{-4} M L^{-1}, respectively, so the reaction rate constant (*k*) for this complex can be calculated as 0.238×10^3 (M L^{-1})$^{-2}$ s^{-1}. The result shows that the order of the reaction with respect to the oxidodiperoxidovanadium complex

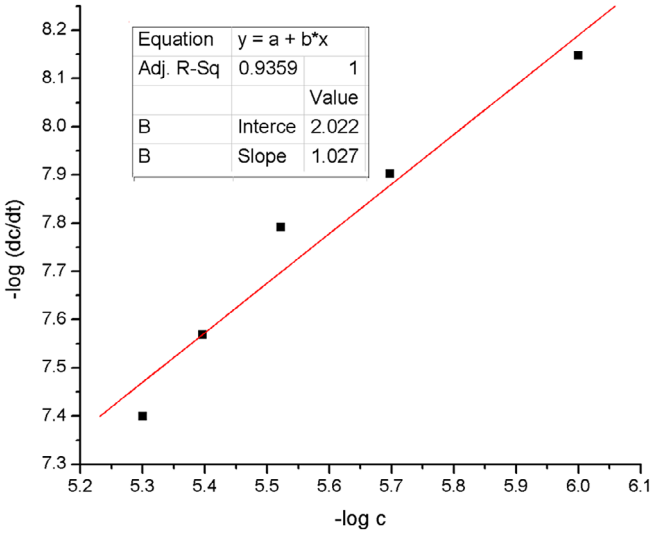

Figure 5. −log(d*c*/d*t*) *vs.* −log *c* (*c* is the concentration of the complex); conditions used: c (phosphate buffer) = 50 mM L^{-1}, pH = 5.0, c(KBr) = 0.4 mol L^{-1}, c(phenol red) = 10^{-4} M L^{-1}.

in bromination reaction is close to 1, confirming the first-order dependence on vanadium species.

The mechanism of action matches the earlier proposition [20, 40, 42]. The bromide ion (Br^-) is oxidized rapidly by the $[VO(O_2)_2N_2]^-$ moiety and converted to the bromonium ion (Br^+) which exists in reaction medium as Br_3^+, Br_2, or HOBr [43]. Attack of a bromide ion at one of the protonated peroxido atoms and the uptake of a proton from the medium leads to the generation of hypobromous acid (HOBr) followed by restoration of the ion to its native state by the attack of H_2O_2 on the intermediate [40]. The *in situ* generated bromonium ion in the form of hypobromous acid attacks the organic substrate (phenol red) to form the corresponding brominated derivative (here bromophenol blue). We compared the catalytic activity and kinetic data of some complexes reported previously (Table 3). It is found that peroxidovanadium complexes show higher catalytic activity than those of oxidovanadium complexes such as **2** and **3** [24], probably because of its built-in peroxido moiety [44]. Therefore, it maybe considered that the catalytic activity of the complexes may have a connection with their structural motifs.

3.4.2. Effect of the concentration of H_2O_2 on bromination

The dependence of the concentration of H_2O_2 on the catalytic bromination reaction has been calculated to develop a new H_2O_2 detection method. The results show that the absorbance at 592 nm depends linearly on the concentration of H_2O_2 along with the formation of bromophenol blue (Figure 6). The present work reveals that the detection limit of H_2O_2 concentration is 0.1594 mol L^{-1}, approximately 0.16 mol L^{-1} (Figure 7). It indicates that above this concentration limit the catalyst can detect H_2O_2. This value is much lower than previously reported literature values [25, 26]. We have compared our work with previously reported values that are presented in Table 4. Although, the earlier report by Liu and coworkers [25]

Table 3. Comparisons of the kinetic data for the complexes.

Complexes	k(M $L^{-1})^{-2}s^{-1}$	Ref.
1	1.5754×10^3	[30(b)]
2	0.238×10^3	This work
3	0.187×10^3	[24]
4	0.184×10^3	[25]

1 $Na[VO(O_2)_2(C_{10}H_8N_2)]\cdot8H_2O$; **3** $(VO)_2(2,2'\text{-bipy})_2(bta)(H_2O)_2$; **4** $(VO)_2(1,10\text{-phen})_2(bta)(H_2O)_2$.

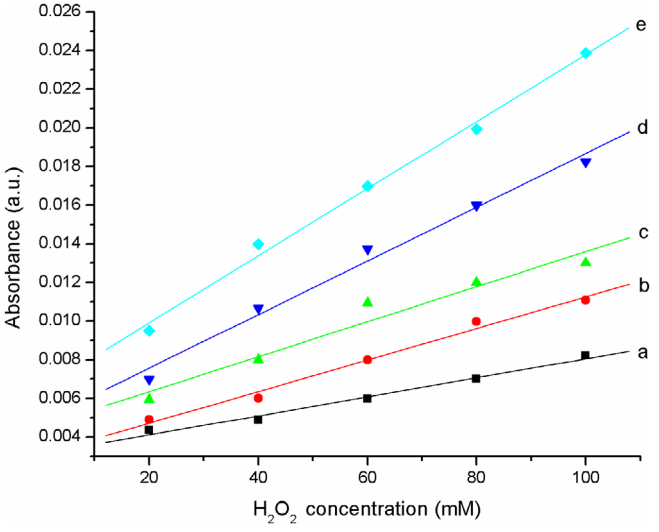

Figure 6. The measurable absorbance dependence on the concentration of H_2O_2 at 10 min intervals of the complex. Condition used: pH 5.0, c(KBr) = 0.4 M L^{-1}, c(complex **1**) = 0.02 M L^{-1}, c(phenol red) = 10^{-4} M L^{-1}. c(H_2O_2/M L^{-1}) = 0.2, 0.4, 0.6, 0.8, 1.0. (a: 35 min; b: 45 min; c: 55 min; d: 65 min; e: 75 min).

presented a lower detection limit of H_2O_2, they used metal clusters instead of metal complexes.

Hence, the above observations suggest that the present complex maybe used as a simple system for the detection or sensing of H_2O_2 through the bromoperoxidation catalysis of phenol red, and possesses potential diagnostic property for sensing and estimation of H_2O_2.

3.5. Kinetic stability of the complex

Since the bromoperoxidation was monitored spectrometrically until complete conversion of the substrate over 8 h, the kinetic study of the decomposition of the complex for ~15 h in aqueous buffer solution was carried out to prove the stability of the complex (Figure S1) during conversion of phenol red. Electronic absorption spectra of the complex solution were recorded after 3 min intervals to see the change in absorbance with respect to time. The absorbance values at 271 nm were plotted against respective time and fitted in a first-order rate equation, from which the dissociation constant (K_{diss}) was obtained. The dissociation constant (K_{diss}) was $(1.889 \pm 0.02)\times10^{-5}$ s^{-1}. This clearly establishes the stability of the complex during the course of the reaction.

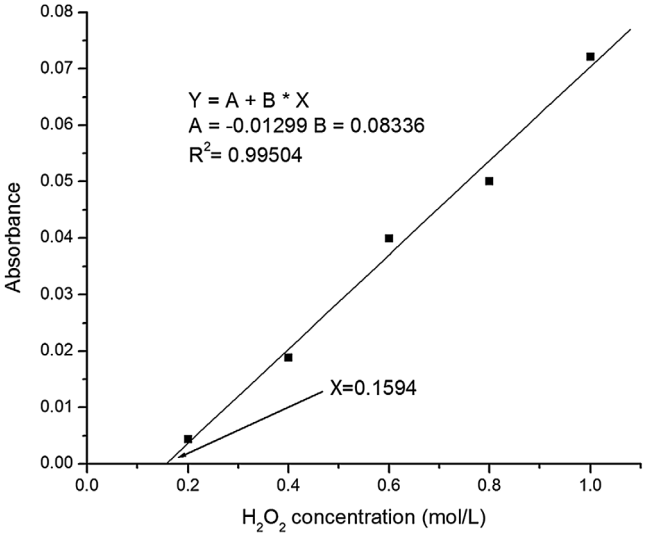

Figure 7. The linear calibration plot of the absorbance at 592 nm on the concentration of H_2O_2 after 35 min for **1** as catalyzer.

Table 4. Comparative study of H_2O_2 detection.

Name of compound	Detection limit value (mol/ L^{-1})	Ref.
[VO(Tp)(pz)(SCN)]·1/2CH_2Cl_2	0.48	[25]
[VO(Tp)(pzTp)]·2H_2O	1.1	[25]
$(VO)_2$(1,10-phen)$_2$(bta)$(H_2O)_2$	1.0	[24]
[$VO(O_2)_2$(phen)]$(NH_4)(H_2O)_2$	0.16	This work

4. Conclusion

The vanadium(V) oxidodiperoxido complex with 1,10-phenanthroline ligand has been synthesized and structurally characterized. The complex exhibits good vanadium-based bromoperoxidase activity (VBrPO) in the model system and also presents a sensitive optical response in the presence of a low concentration of H_2O_2. So the compound can be used as a H_2O_2 sensor as well. A comparison of literature values indicates that the present complex is a better candidate for H_2O_2 detection via bromination of phenol red. Based on the results, we expect that a simple and sensitive H_2O_2 detection device will be exploited in the future. Further research on the potential application of the H_2O_2 detection is ongoing.

Acknowledgements

HA is thankful to UGC for providing Junior Research Fellowship. Thanks are due to Jadavpur University for facilities. The authors are thankful to Dr. Kuntal Pal, University of Calcutta, for assistance.

Disclosure statement

No potential conflict of interest was reported by the authors.

References

[1] H. Vilter. *Bot. Mar.*, **26**, 451 (1983).
[2] H. Vilter. *Phytochemistry*, **23**, 1387 (1984).
[3] D. Rehder. *Coord. Chem. Rev.*, **182**, 297 (1999).
[4] A. Butler. *Coord. Chem. Rev.*, **187**, 17 (1999).
[5] A. Butler, M. Sandy. *Nature*, **460**, 848 (2009).
[6] S. Amachi. *Microb. Environ.*, **23**, 269 (2008).
[7] S. La Barre, P. Potin, C. Leblanc, L. Delage. *Mar. Drugs*, **8**, 988 (2010).
[8] C. Paul, G. Pohnert. *Nat. Prod. Rep.*, **28**, 186 (2011).
[9] J.M. Winter, B.S. Moore. *J. Biol. Chem.*, **284**, 18577 (2009).
[10] L.C. Blasiak, C.L. Drennan. *Acc. Chem. Res.*, **42**, 147 (2009).
[11] C. Wagner, M. El Omari, G.M. König. *J. Nat. Prod.*, **72**, 540 (2009).
[12] R. Wever, W. Hemrika, *Vanadium Haloperoxidases*. In *Handbook of Metalloproteins,* J.W. Sons (Ed.), pp. 1–12, (2006).
[13] C. Leblanc, C. Colin, A. Cosse, L. Delage, S. La Barre, P. Morin, B. Fiévet, C. Voiseux, Y. Ambroise, E. Verhaeghe, D. Amouroux, O. Donard, E. Tessier, P. Potin. *Biochimie*, **88**, 1773 (2006).
[14] F.C. Küpper, L.J. Carpenter, G.B. McFiggans, C.J. Palmer, T.J. Waite, E.-M. Boneberg, S. Woitsch, M. Weiller, R. Abela, D. Grolimund, P. Potin, A. Butler, G.W. Luther, P.M.H. Kroneck, W. Meyer-Klauckel, M.C. Feiters. *Proc. Natl Acad. Sci.*, **105**, 6954 (2008).
[15] S.L. Neidleman, J.L. Geigert. *Biohalogenation*., Ellis Horwood Ltd. Press, New York, NY (1986).
[16] (a) A. Butler, M.J. Clague, G.E. Meister. *Chem. Rev.*, **94**, 625 (1994); (b) A. Butler, M.J. Clague, *Modeling Vanadium Bromoperoxidase Oxidation of Halides by Peroxovanadium(V)Complexes*. In *Mechanistic Bioinorganic Chemistry*, pp. 329–349 (1996).
[17] (a) H. Vilter, *Vanadium Dependent Haloperoxidase*. In *Metal Ions in Biological Systems H. Sigel and A. Sigel, Marcel Dekker (Ed.) Vanadium and its Role in Life*, vol. 31, pp. 231–247, New York (1995);(b) K.E. Liu, A.M. Valentine, D. Qiu, D.E. Edmondson, E.H. Appelman, T.G. Spiro, S.J. Lippard. *J. Am. Chem. Soc.*, **117**, 4997 (1995).
[18] Y.H. Xing, Z. Sun, W. Zou, J. Song, K. Aoki, M.F. Ge. *J. Struct. Chem.*, **47**, 913 (2006).
[19] Y.H. Xing, K. Aoki, Z. Sun, M.F. Ge, S.Y. Niu. *J. Chem. Res.*, **108**, 2 (2007).
[20] (a) S. Patra, S. Chatterjee, T.K. Si, K.K. Mukherjea. *Dalton Trans.*, **42**, 13425 (2013); (b) Y.H. Xing, Y.H. Zhang, Z. Sun, L. Ye, Y.T. Xu, M.F. Ge, B.L. Zhang, S.Y. Niu. *J. Inorg. Biochem.*, **101**, 36 (2007); (c) U. Saha, T.K. Si, P.K. Nandi, K.K. Mukherjea. *Inorg. Chem. Commun.*, **38**, 43 (2013); (d) S. Patra, K.K. Mukherjea. *Chemistry Select*, **2**, 521 (2017).
[21] A. Asthana, K.H. Lee, S. Shin, J. Perumal, L. Butler, S. Lee, D. Kim. *Biomicrofluidics*, **5**, 024117 (2011).
[22] L.-C. Jiang, W.-D. Zhang. *Electroanalysis*, **21**, 988 (2009).
[23] R. Zhang, X. Zhang, F. Bai, C. Chen, Q. Guan, Y. Hou, X. Wang, Y. Xing. *J. Coord. Chem.*, **67**, 1613 (2014).
[24] R. Zhang, J. Liu, C. Chen, Y. Xing, Q. Guan, Y. Hou, F. Bai. *Spectrochim. Acta Part A*, **115**, 476 (2013).
[25] (a) S. Liu, J.Q. Tian, L. Wang, Y.W. Zhang, Y.L. Luo, H.Y. Li, A.M. Asiri, A.O. Al-Youbi, X.P. Sun. *ChemPlusChem.*, **77**, 541 (2012); (b) Q. Chen, T. Lin, J. Huang, Y. Chen, L. Guo, F. Fu. *Anal. Methods*, (2018). doi:10.1039/c7ay02819a.
[26] G.H. Jeffery, J. Bassett, J. Mendham, R.C.D. Addison. *Vogel's Text Book of Quantitative Chemical Analysis*, 5th Edn., Wesley Longman Limited, UK (1989).
[27] (a) Bruker, APEX 2, SAINT, XPREP, Bruker AXS Inc., Madison, Wisconsin, USA (2007); (b) N. Walker, D. Stuart. *Acta Crystallographica Section A Foundations of Crystallography*, **39**, 158 (1983); (c) G.M. Sheldrick, *SAINT, Version 6.02, SADABS, Version 2.03*, Bruker AXS Inc., Madison, WI (2002).
[28] (a) G.M. Sheldrick. *Acta Cryst.*, **A64**, 112 (2008); (b) C.F. Macrae, P.R. Edgington, P. McCabe, E. Pidcock, G.P. Shields, R. Taylor, M. Towler, J. van de Streek. *J. Appl. Cryst.*, **39**, 453 (2006); (c) L.J. Farrugia. *J. Appl. Cryst.*, **45**, 849 (2012).
[29] E. Verhaeghe, D. Buisson, E. Zekri, C. Leblanc, P. Potin, Y. Ambroise. *Anal. Biochem.*, **379**, 60 (2008).
[30] (a) N. Vuletic, C. Djordjevic. *J. Chem. Soc., Dalton Trans.*, **1137**, (1973); (b) C. Chen, Z. Rui, W. Xuan, C. Yunzhu, B. Fengying, Z. Xiaoxi, L. Guanghu, S. Zhan, X. Yongheng. *Chin. J. Appl. Chem.*, **30**, 1453 (2013).

[31] (a) H. Szentivanyi, R. Stomberg. *Acta Chem. Scand.*, **37**, 553 (1983); (b) A.S. Barakat, A.S. Gaballa, S.F. Mohammed, S.M. Teleb. *Spectrochim. Acta, Part A*, **62**, 814 (2005).
[32] V.S. Sergienko. *Crystallogr. Rep.*, **49**, 401 (2004).
[33] A.D. Keramidas, S. Miller, O.P. Anderson, D.C. Crans. *J. Am. Chem. Soc.*, **119**, 8901 (1997).
[34] (a) W.P. Griffith, T.D. Wickins. *J. Chem. Soc. A*, **400**, (1968); (b) L.W. Amos, D.T. Sawyer. *Inorg. Chem.*, **11**, 2692 (1972).
[35] P. Schwendt. *Chem. Papers*, **45**, 305 (1988).
[36] G.J. Colpas, B.J. Hamstra, J.W. Kampf, V.L. Pecoraro. *J. Am. Chem. Soc.*, **118**, 3469 (1996).
[37] (a) A. Messerschmidt, R. Wever. *Proc. Natl. Acad. Sci. U.S.A.*, **93**, 392 (1996); (b) A. Messerschmidt, L. Prade, R. Wever. *Biol. Chem.*, **378**, 309 (1997); (c) C. Selbodnick, B.J. Hamstra, V.L. Pecoraro. *Struct. Bonding*, **89**, 51 (1997); (d) M.J. Clague, N.L. Keder, A. Butler. *Inorg. Chem.*, **32**, 4754 (1993).
[38] (a) A.G.J. Ligtenbarg, R. Hage, B.L. Feringa. *Coord. Chem. Rev.*, **237**, 89 (2003); (b) C. Kimblin, X. Bu, A. Butler. *Inorg. Chem.*, **41**, 161 (2002).
[39] (a) O. Brotolini, V. Conte. *J. Inorg. Biochem.*, **99**, 1549 (2005); (b) S. Rougei, P. Carloni. *J. Phys. Chem. B*, **110**, 3747 (2006); (c) J.Y. Kravitz, V.L. Pecoraro. *Pure Appl. Chem.*, **77**, 1595 (2005).
[40] (a) T.K. Si, M.G.B. Drew, K.K. Mukherjea. *Polyhedron*, **30**, 2286 (2011); (b) U. Saha, K.K. Mukherjea. *RSC Adv.*, **5**, 94462 (2015); (c) V. Conte, B. Floris. *Inorg. Chim. Acta*, **363**, 1935 (2010).
[41] T.N. Mandal, S. Roy, A.K. Barik, S. Gupta, R.J. Butcher, S.K. Kar. *Polyhedron*, **27**, 3267 (2008).
[42] T.K. Si, S.S. Paul, M.G.B. Drew, K.K. Mukherjea. *Dalton Trans.*, **41**, 19 (2012).
[43] (a) A.G.J. Ligtenbarg, R. Hage, B.L. Feringa. *Coord. Chem. Rev.*, **237**, 89 (2003); (b) D. Rehder, G. Santoni, G.M. Licini, C. Schulzke, B. Meier. *Coord. Chem. Rev.*, **237**, 53 (2003); (c) V. Kraehmer, D. Rehder. *Dalton Trans.*, **41**, 5225 (2012).
[44] E. Palmajumder, S. Patra, M.G.B. Drew, K.K. Mukherjea. *New J. Chem.*, **40**, 8696 (2016).